ELSEVIER

Biochimica et Biophysica Acta 1282 (1996) 293–302

BBA Biochimica et Biophysica Acta

Monovalent cations differentially affect membrane surface properties and membrane curvature, as revealed by fluorescent probes and dynamic light scattering

Ruud Kraayenhof [a,*], Geert J. Sterk [b], Harro W. Wong Fong Sang [a], Klaas Krab [a], Richard M. Epand [c]

[a] *Institute of Molecular Biological Sciences, BioCentrum Amsterdam, Vrije Universiteit, De Boelelaan 1087, 1081 HV, Amsterdam, The Netherlands*
[b] *Byk Nederland B.V., P.O. Box 61, 1160 AB, Zwanenburg, The Netherlands*
[c] *Department of Biochemistry, McMaster University Health Sciences Centre, 1200 Main Street West, Hamilton, Ontario, L8N 3Z5, Canada*

Received 28 February 1996; revised 1 April 1996; accepted 1 April 1996

Abstract

The effects of monovalent cations on the interfacial electrostatic potential (ψ_d), hydrodynamic shear boundary distance (d_s), and membrane curvature were studied in large unilamellar phospholipid and galacto/sulfolipid liposomes containing different fractions of negatively charged lipids. The differential effects of alkali metal ions on ψ_d could be accurately determined at physiological surface charge densities with a surface-anchored fluorescent probe. Li^+ and Na^+ more effectively decrease ψ_d and exhibit higher association constants (K_{as}) than K^+ and Cs^+. These two groups of cations display qualitatively different perturbations of the interfacial structure. Combining K_{as} values with the electrokinetic (ζ) potentials yielded the respective d_s values. At low ionic strength d_s more substantially increases with Li^+ or Na^+ than with K^+ or Cs^+. Increasing surface charge density causes increased membrane curvature in the presence of K^+ or Cs^+, but this is largely prevented by Li^+ or Na^+. Membrane binding of the amphiphilic cation acridine orange decreases surface charge and membrane curvature more extensively than H_3O^+, Li^+, and Na^+. The differential interface-perturbing behavior of monovalent cations is discussed with regard to their different hydration tendencies that will modulate the extent and stability of the hydrogen-bond network along the charged membrane surface.

Keywords: Surface potential; Membrane hydration; Hydrodynamic shear boundary; Membrane curvature; Monovalent cation association; Fluorescence probe

1. Introduction

The surfaces of essentially all biological membranes are negatively charged, mainly due to the net negative charges of lipid head groups. The molar fraction of these lipids ranges from 5 to 25%, corresponding to surface charge densities between about -0.01 and -0.05 C m^{-2}. This results in negative electrostatic potentials which decline with distance from the membrane surface. The shape of this potential profile is adequately described by the Gouy-Chapman-Stern theory and depends on the concentration and type of the electrolytes in the adjacent aqueous phase (see reviews of McLaughlin, [1,2]). The existence of a negative surface potential is of crucial importance for a diversity of membrane structural and functional aspects [2–6]. A feature of the charged interface that may be of general significance for these phenomena is that it promotes the formation of a stable hydration layer of oriented water molecules [7] that may stabilize the lipid head-group region [8]. Although it has been amply demonstrated that there are large amounts of water bound at the membrane surface and that large free energy changes are involved with the dehydration of membrane lipids and proteins [9,10] relatively little is known about the structural organization and properties of this interfacial water of hydration.

Abbreviations: AO, acridine orange (3,6-dimethylaminoacridine); DGDG, digalactosyl diacylglycerol; Hepes, *N*-(2-hydroxyethyl)piperazine-*N'*-(2-ethanesulfonic acid); LUVETs, large unilamellar vesicles prepared by extrusion technique; MGDG, monogalactosyl diacylglycerol; PAME, phosphatidic acid monomethyl ester; PC, phosphatidylcholine; PS, phosphatidylserine; SQDG, sulfoquinovosyl diacylglycerol; U-2, 4-heptadecyl-7-hydroxycoumarin; U-6, 4-[*N,N*-dimethyl-*N*-(n-tetradecyl)ammoniummethyl]-7-hydroxycoumarin chloride.

* Corresponding author. Fax: +31 20 4447157; e-mail: kr@bio.vu.nl.

PII S0005-2736(96)00069-7

Cations are attracted by negatively charged interfaces, anions are repelled. However, there are differences among ions in their binding affinity as well as in the extent of partitioning into or exclusion from the hydration layer, i.e. the phenomenon of preferential hydration, extensively studied for hydrated proteins (cf. [11] and refs. therein). For example, effects on the bilayer to hexagonal phase transition of both mono- and divalent ions can be explained by ion binding and preferential hydration [12]. Eisenberg et al. [13] have demonstrated that, in addition to their electrostatic screening, monovalent cations bind to multilamellar PC/PS vesicles with decreasing association constant in the sequence Li^+, Na^+, NH_4^+, K^+, Rb^+, Cs^+, tetraethylammonium$^+$ and tetramethylammonium$^+$. Monovalent cations may perturb the hydration layer and thereby the membrane stability to different extents, depending on their own hydration tendency [14,15]. Among the alkali metal ions Li^+ and Na^+ belong to the group of so-called (water) 'structure makers', together with H^+ (or rather the hydronium ion H_3O^+), OH^-, F^-, Mg^{2+}, Ca^{2+}, some large amphiphilic cations such as aminoacridines, and disaccharides. In contrast, K^+, Rb^+ and Cs^+ are called 'structure breakers', together with NH_4^+, Cl^- and most other anions, and urea.

The older concept of structure making vs. breaking is now considered somewhat ambiguous in view of more sophisticated measurements and models [16]. However, some pertinent differences between these categories are worth mentioning. The residence time of hydration water is much longer with structure makers than with structure breakers [17], the first increase the viscosity of the surrounding solvent while the second decrease it [18]. It was also observed that Li^+ (but not K^+) effectively increases the hydrodynamic shear boundary distance of charged colloidal particles [19]. We have recently noticed that liposomes extruded in the presence of 10 mM KCl assume a smaller vesicle diameter (increased membrane curvature) with increasing surface charge density [20]. Under similar conditions, the polarity near the lipid head groups increases, the head groups show greater mobility [21], and the number of head group-bound water molecules decreases [22]. Also noteworthy is the earlier work of Rigaud and Gary-Bobo [23] on lateral diffusion rates of alkali metal ions in the PC/water interface, which clearly depend on the extent of membrane hydration, but diffusional selectivity also depends on the hydration tendency of the cations themselves. Extensive surface hydration is characterized by a strong repulsive hydration force (distinct from electrostatic and Van der Waals forces) which is increased by alkali metal ions in the sequence $Li^+ > Na^+ > K^+ > Cs^+$ [24].

In view of these considerations we have compared in this study the effects of the monovalent cations Li^+, Na^+, K^+, and Cs^+ on the interfacial potential (ψ_d) and post-extrusion vesicle size (membrane curvature) of large unilamellar liposomes with increasing surface charge density. We have recently introduced membrane-anchored ('float-like') fluorescent probes for accurate determination of ψ_d as function of distance or surface charge density [20]. The reporter groups of these probes are located at different distances from the membrane surface. One of the new probes, U-6, is applied here to study the effects of these cations on ψ_d. This probe senses ψ_d at a distance of about 0.64 nm from the plane of maximal (surface) potential (ψ_0). In some cases we used the known probe U-2 [4,25] with a sensor distance of 0–0.15 nm. A fitting procedure based on the Gouy-Chapman-Stern theory yielded the association constants (K_{as}) for the cations, and by combining these with electrokinetic (ζ) potential measurements under the same conditions, we determined the respective distances of the hydrodynamic shear boundary (at which the ζ potential is sensed). For comparison we have also examined the binding and interface-perturbing effects of acridine orange (AO) as an example of a family of large amphiphilic monovalent cations that are known to interact strongly with negatively charged and hydrated polymers and interfaces [15,26].

Two types of large unilamellar liposomes with different lipid composition were used. One type contains PC with variable fractions of the monomethylester of phosphatidic acid (PAME) as a simple, monovalent negatively charged lipid (in some cases PS was tested). The other contains a 2:1 mixture of the uncharged galactolipids MGDG and DGDG with variable fractions of the monovalent sulfolipid SQDG. These two liposome preparations may serve as simplified models for animal and plant membranes, respectively. The fractions of charged lipids were kept below 30 mol% so as to mimic the surface charge density range of native biomembranes.

2. Materials and methods

2.1. Preparation of liposomes

Purity of the commercial lipids PC, PAME, DGDG, MGDG and SQDG was verified by TLC. First, multilamellar vesicles of different PC/PAME or MGDG-DGDG/SQDG mixtures were prepared by mixing the lipids in chloroform/methanol (9:1), rotational evaporation of the solvent until dryness, vortex mixing and 10 freeze-thaw cycles of the suspension in media of different composition, as indicated in the figure legends. The galactolipids MGDG and DGDG were always present in a molar ratio of 2:1. LUVETs were prepared by stepwise extrusion of the multilamellar vesicles as described by Mayer et al. [27]. The extrusion in a modified stainless steel version of the Extruder from Lipex Biomembranes Inc. (Vancouver, BC, Canada) involved successively 5 cycles through 800 nm-pore polycarbonate membranes (Nuclepore, Costar Europe) and 10 cycles through 400 nm-pore membranes. The final liposome diameters may

deviate from 400 nm, as indicated under Results. For each LUVET preparation fresh polycarbonate membranes (in stacks of 2) and polyethylene supporting filters (36 μm pores, thickness 2.5 mm) were used. The presented experiments were carried out with LUVETs prepared on the same day. Final concentration of total lipid was 0.25 mg lipid ml^{-1}. (For further details see [20].)

2.2. Extrusion and test media

For measurements of the effects of increasing monovalent cation concentration ψ_d and ζ potential and vesicle size, the LUVETs were incubated in 0.5 mM EDTA, 2 mM Hepes, titrated with tetramethylammonium hydroxide (for pH, see the legends to the figures), because the tetramethylammonium cation does not significantly affect the ζ potential [13]. Although prior addition to the vesicles of 0.5 mM EDTA, to bind possible residual traces of bivalent cations, did not affect the ψ_d and ζ potentials, we have added this compound routinely before extrusion.

2.3. Fluorescent measurements and probes

Fluorescence spectra and measurements of time-dependent intensity changes were recorded with a SLM-Aminco SPF-500 fluorometer. The fluorimetric determinations of the pK_a values of the U-2 and U-6 probes were performed by acid-base titrations, started at the low pH end and performed as fast as possible. Fluorescence lifetime measurements on AO were performed with a LS-100 multipurpose fluorimeter (Photon Technology International, London, Ontario, Canada).

The structures of U-2 and U-6, and the synthesis and structural analysis of the latter probe are described in a preceding paper [20]. U-6 is now commercially available from Molecular Probes, Eugene, OR. Binding of U-2 and U-6 to the LUVETs before experiments was carried out as described earlier [20]. AO binding was directly monitored fluorimetrically in the final liposome incubation. We have shown earlier that in binding experiments the quenched fraction matches the fraction which disappeared from the medium [28]. In most experiments a molar probe/total lipid ratio of 1:165 or lower is used for U-2 and U-6 (probe concentrations were about 2 μM unless stated otherwise). At this ratio there was no detectable effect on the ζ potentials.

2.4. Doppler-electrophoretic light scattering analysis

The ζ potentials, derived from the electrophoretic mobilities, and the average hydrodynamic vesicle diameters of the LUVETs were obtained with a DELSA 440 apparatus (Coulter Electronics, Hialeah, FL) which employs a four-angle detection of the Doppler shift of the frequency of scattered laser light. The apparatus also measures the electric conductance of the medium and applies the data in calculations. Medium viscosity was checked with a Schott (Mainz, Germany) viscosimeter.

2.5. Calculations and simulations

The calculation of the charge densities of LUVETs was based on the assumptions that both PC and PAME molecules (fully hydrated) occupy a surface area of 70 $Å^2$ and that this area is 75 $Å^2$ for the galactolipids and sulfolipid. The respective membrane surface potentials (ψ_0) were calculated according to [1]. The local electrostatic potential at distance d from the membrane surface (ψ_d), i.e. at the position of the coumarin-hydroxyl groups of the probes U-6 and U-2, is calculated from the difference of the apparent pK_a values with those at (extrapolated) zero surface charge density (pK_a^0), also corresponding to the difference between the pH at distance d (pH_d) and the bulk medium pH (pH_b), according to the relation [25]:

$$\psi_d = -2.3RT/F(pK_a - pK_a^0)$$
$$= -2.3RT/F(pH_b - pH_d)\ mV$$

in which $RT/F = 25.69$ mV at 25°C [1]. The theoretical ψ_d profiles were simulated by a spreadsheet protocol, using the equations of the Gouy-Chapman-Stern theory, based on the non-linear Poisson-Boltzmann relation (for equations see Refs. [1,2,13,20,29]).

2.6. Chemicals

All chemicals were of analytical grade. PC, PS and PAME were obtained from Sigma (St. Louis, MO, USA). DGDG, MGDG and SQDG were obtained from Serdary Research Laboratories (London, Ontario, Canada) and from Lipid Products, Nutfield Nurseries (South Nutfield, Surrey, UK). 4-Heptadecyl-7-hydroxycoumarin (U-2) was obtained from Molecular Probes (Eugene, OR, USA). AO was obtained from Chroma Gesellschaft (Köngen, Germany).

3. Results

3.1. pH dependence of ζ potential and liposome size of LUVET preparations

In order to characterize the membrane surface properties of the two LUVET preparations, containing different fractions of charged lipids, the ζ potentials and average hydrodynamic vesicle diameters were measured as function of pH. Fig. 1 shows the ζ potentials for both types of liposomes with increasing fractions of PAME or SQDG. In the absence of added negatively charged lipid the liposomes are usually slightly negative, especially in the case of PC. The possible reasons for this are discussed elsewhere [20,30]. Below pH 5 the pure PC liposomes become

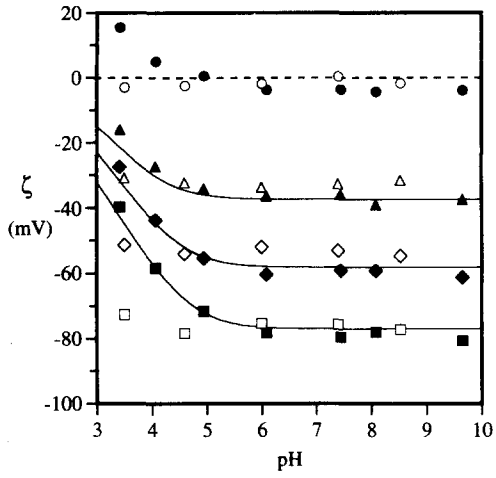

Fig. 1. pH dependence of the electrokinetic (ζ) potentials of PC/PAME and MGDG-DGDG/SQDG liposomes with different surface charge density. The medium contained 10 mM KCl, 2 mM Hepes (pH as indicated), 0.5 mM EDTA, and 0.25 mg lipid per ml. Closed symbols: PC/PAME liposomes; open symbols: MGDG-DGDG/SQDG liposomes; the molar fractions of the negatively charged lipids were: 0% (●,○), 5% (▲,△), 10% (◆,◇), or 20% (■,□).

positively charged, as expected. In the monomethyl ester of PA only its low-pK_a phosphoryl group can be protonated. Fig. 1 also displays the curves simulated for 5, 10 and 20% PAME with a single pK_a of 3.0 [31], and assuming zero charge of PC above pH 6. The deviations of the data from these curves can be explained by the protonation of the PC phosphoryl group, retaining the positive choline. In the case of the galacto/sulfolipid vesicles one observes a fairly constant ζ potential in this pH range because the pK_a of the sulfonic acid group of SQDG is lower than 0.

The average vesicle diameters of the PC/PAME liposomes under the same conditions are depicted in Fig. 2. As

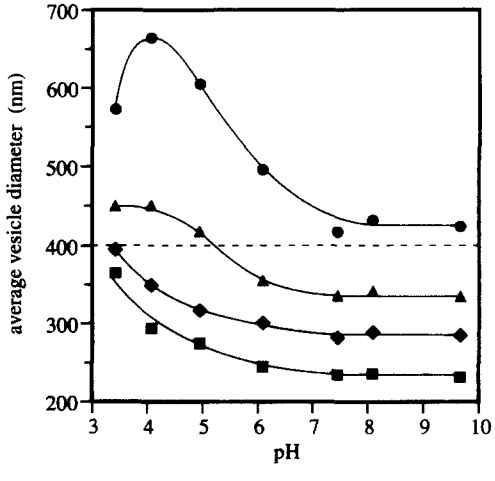

Fig. 2. pH dependence of the average hydrodynamic diameters of PC/PAME liposomes. Conditions were as in Fig. 1. The molar fractions of the negatively charged lipids were: 0% (●), 5% (▲), 10% (◆), or 20% (■).

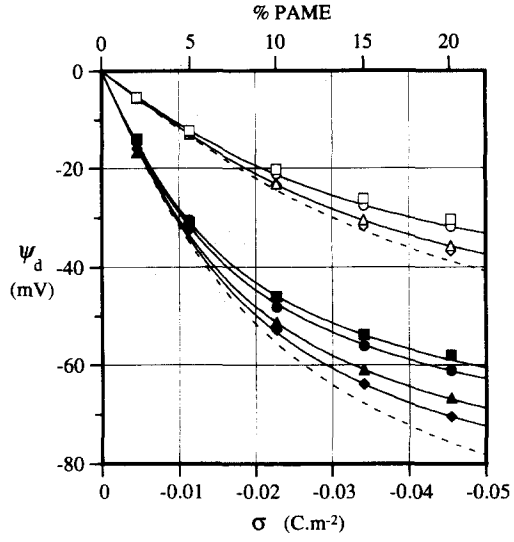

Fig. 3. The effect of monovalent cations on the interfacial potentials (ψ_d), of PC/PAME liposomes obtained with the fluorescent probe U-6, as function of membrane surface charge density. The medium contained 2 mM Hepes/TMAOH, pH 7.4, 0.5 mM EDTA, 0.25 mg lipid per ml, and salts as indicated below. Curves were simulated for ψ_d (at $d = 0.64$ nm) with a flexible spreadsheet protocol based on the equations given in [13], and K_{as} was varied to best fit. In the 50 mM series curves are only shown for Na^+ and K^+. Dashed lines are simulated for $K_{as} = 0$. Standard deviations ($n = 3$ or 4) varied between 2.9 and 5.2 mV (error bars omitted for better clarity). Closed symbols: 10 mM Cl^- salts; open symbols: 50 mM Cl^- salts. Cations were: Cs^+ (◆,◇), K^+ (▲,△), Na^+ (●,○), or Li^+ (■,□).

reported earlier [20], vesicle size decreases with increasing surface charge density (at pH 7.4 in 10 mM KCl). The average diameter of the (slightly negative) pure PC liposomes is usually somewhat larger (max. 5%) than the average extrusion filter pore diameter above pH 7.4. However, at lower pH this size increases, probably by vesicle fusion or aggregation, and is maximal around the isoelectric point of the liposomes. At higher surface charge densities a smaller size increase is also apparent at lower pH. The galacto/sulfolipid LUVETs showed a similar decrease of vesicle size with increasing SQDG fraction. Only in the absence of SQDG the liposomes showed a size increase (to 430–500 nm) at pH 6 and below.

3.2. Alkali metal ion effects on interfacial potential at different surface charge densities; estimation of association constants

LUVET preparations with increasing surface charge density were labeled with the probe U-6, and ψ_d values were determined by fluorimetric titrations from the upward shifts of the apparent pK_a values of the coumarin fluorophore. In Fig. 3 the results are compiled for PC/PA liposomes in 10 and 50 mM Li^+, Na^+, K^+, and Cs^+ (chlorides). There were only small additional effects at salt concentrations of 100 and 200 mM (not shown). Very similar results were obtained with the galacto/sulfolipid

Table 1
Estimated association constants (K_{as}) for monovalent cation adsorption in PC/PAME and MGDG-DGDG/SQDG liposomes [a]

Monovalent cation	Concn. (mM)	K_{as} (M^{-1}) ± SD ($n = 3$)	
		PC/PAME	MGDG-DGDG/SQDG
Li^+	10	3.82 ± 0.53	3.14 ± 0.46
	50	1.29 ± 0.12	1.11 ± 0.10
	100	0.89 ± 0.07	0.82 ± 0.09
Na^+	10	2.79 ± 0.42	2.68 ± 0.51
	50	0.95 ± 0.06	0.96 ± 0.12
	100	0.78 ± 0.06	0.69 ± 0.07
K^+	10	1.13 ± 0.23	0.92 ± 0.21
	50	0.28 ± 0.02	0.22 ± 0.07
	100	0.18 ± 0.02	0.16 ± 0.05
Cs^+	10	0.51 ± 0.05	0.48 ± 0.07
	50	0.16 ± 0.07	0.16 ± 0.05
	100	0.11 ± 0.03	0.14 ± 0.05

[a] Data were obtained from experiments as described in Fig. 3.

LUVETs. Despite the practical impossibility to obtain all data points per fixed charge density with a single batch of LUVETs the results were remarkably reproducible, even within this range of relatively low charge densities. When considering their effects on ψ_d, Li^+ and Na^+ form a more effective group than K^+ and Cs^+. The cation adsorption effects were simulated for the U-6 fluorophore distance of 0.64 nm [20] and varying K_{as}, until a best fit to the data was obtained (solid curves in Fig. 3). Table 1 shows that the K_{as} values thus obtained in 10, 50 and 100 mM electrolyte are very similar in both types of liposomes. In the presence of only the Hepes-TMAOH buffer the data (not shown) closely followed the dashed curves which were simulated for $K_{as} = 0$.

3.3. Alkali metal ion effects on electrokinetic potential at different surface charge densities; estimation of shear boundary distance

Under the same conditions as the ψ_d measurements we have investigated the different cation effects on the ζ potentials of the same series of LUVETs. The results are shown in Fig. 4 for the PC/PAME liposomes. Now, the simulations were based on the K_{as} values derived from the ψ_d measurements in Fig. 3, and values for the distance parameter d_s (indicating the position of the hydrodynamic plane of shear) were varied until a best fit to the data (between 10 and 20% PAME) was obtained (solid curves in Fig. 4). At 10 mM Li^+, Na^+, K^+ and Cs^+ the optimal values for d_s were 0.40, 0.38, 0.32, and 0.31 nm, respectively; at 50 mM salt these values were 0.27, 0.26, 0.22 and 0.21 nm, respectively (s.d. in all cases less than 8%). Considering the precision level of the ψ_d and ζ potential measurements, the values of d_s are significantly different between the Li^+-Na^+ and K^+-Cs^+ groups at 10 mM, and possibly also at 50 mM, but not between the cations within the same group. At higher salt concentrations (100 and 200 mM) d_s was very similar for all ions (0.18 to 0.21 nm) and in good agreement with the earlier suggested 0.2 nm at decimolar salt concentrations [13,32,33]. Results with galacto/sulfolipid and PC/PS liposomes were very similar.

3.4. Monovalent cation concentration dependence of interfacial potential, association constant, and residual surface charge density

The association of monovalent cations with liposomes was investigated in more detail in the concentration range 2 to 100 mM. As an example of these experiments, the titration of Na^+ in galacto/sulfolipid liposomes (10% SQDG) is presented in Fig. 5. In this case we have used the probe U-2 which is more sensitive to cation-induced decrease of ψ_d because of the closer (but less defined) proximity of its fluorophore to the membrane surface. While U-2 has a much higher pK_a than U-6 these experiments were performed at pH 9.1. Note that ψ_d is effectively decreased by low Na^+ concentrations. Fig. 5 also shows the corresponding values for K_{as} and the residual surface charge density after Na^+ binding (σ_{res}) obtained from the Gouy-Chapman-Stern simulations. The apparent K_{as} does not vary so much in the higher concentration range but strongly increases with decreasing Na^+ concentration in the mM range (K_{as} values at 10, 50 and 100 mM Na^+ are similar to those obtained with U-6, shown in Table 1). σ_{res} increases at higher Na^+ concentrations, because of the implicit ion activity-dependence of K_{as}; in

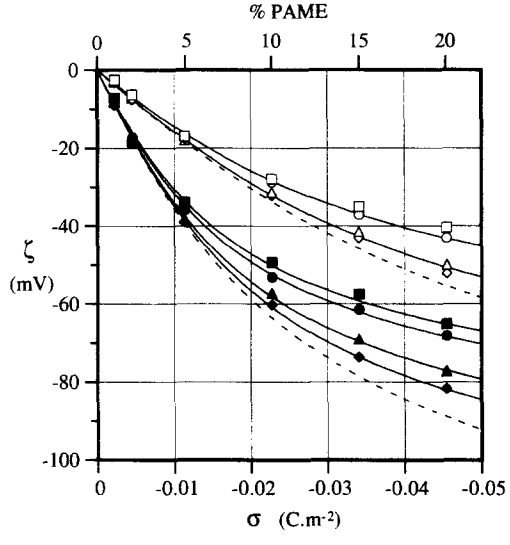

Fig. 4. The effect of monovalent cations on the electrokinetic (ζ) potentials of PC/PAME liposomes as function of membrane surface charge density. Conditions as in Fig. 3. Simulations were based on the values for K_{as} found in the experiments of Fig. 3; d was varied to best fit. S.D. values ($n = 3$) varied between 3.2 and 6.6 mV (error bars omitted for better clarity). Dashed lines indicate the potential profiles for $K_{as} = 0$ and d values for Cs^+ (see text). Closed symbols: 10 mM Cl^- salts; open symbols: 50 mM Cl^- salts. Cations were: Cs^+ (◆,◇), K^+ (▲,△), Na^+ (●,○), or Li^+ (■,□).

this case σ_{res} reaches a constant level of about -0.016 to -0.018 C m^{-2} above 10 mM monovalent salt, for 10 charged lipids, which is in good agreement with values of -0.14 to -0.20 C m^{-2} reported by Ermakov for 100% charged lipids [29].

3.5. Differential cation effects on the average vesicle size obtained after extrusion

Under the same experimental conditions as for the ψ_d and ζ potential measurements the average hydrodynamic vesicle diameters were determined for the LUVETs with different fractions of negatively charged lipid. As shown by Fig. 6, vesicle size decreases with increasing surface charge to almost half its diameter at 20 mol% PAME in PC/PAME liposomes, extruded in the presence of 10 mM KCl or CsCl. However, in the presence of 10 mM LiCl or NaCl this size decrease is much less. At 50 mM of the salts the effects are smaller but the different behavior of the two groups of ions is still obvious. Only a small additional inhibition of size reduction was seen at 100 and 200 mM salt. Very similar results were obtained with the galacto/sufolipid and with PC/PS liposomes in the same range of charge density variation.

We have also measured the combined effects of K^+ and Na^+ ions on post-extrusion vesicle size at 20% PAME. It was found that 10 mM Na^+ combined with K^+ concentrations up to 150 mM yielded roughly the same vesicle size (around 350 nm) as 10 mM Na^+ alone. Therefore, the Na^+ effect is fully dominant, and neither intermediary nor synergistic effects of both cations seem to occur. In addition, the effect of high sucrose concentration was tested. Disaccharides lower the bilayer to hexagonal phase transition temperature [34], counteract dye leakage during lipid phase transition [35], and have a 'structure-promoting' effect [15]. Addition of 0.5 M sucrose to a 2 mM Hepes/10 mM KCl extrusion medium yields about the same vesicle size (290 nm) as 100 mM KCl in the absence of sucrose. Combination of sucrose with Na^+ essentially produced the vesicle sizes obtained with Na^+ alone.

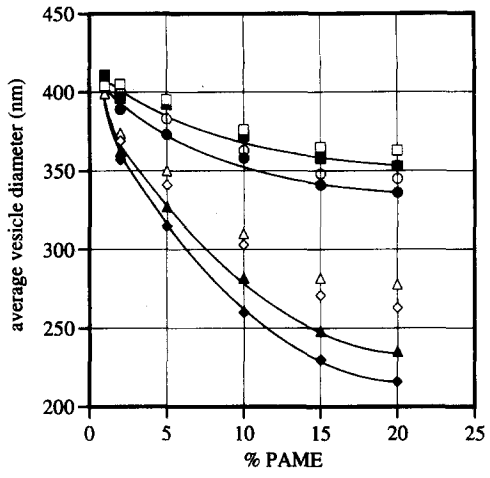

Fig. 6. Differential monovalent cation effects on the average vesicle size obtained after extrusion in PC/PAME liposomes. Extrusion and test media were as in Fig. 3. Closed symbols; 10 mM Cl^- salts; open symbols: 50 mM Cl^- salts. Cations were: Cs^+ (◆,◇), K^+ (▲,△), Na^+ (●,○), or Li^+ (■,□).

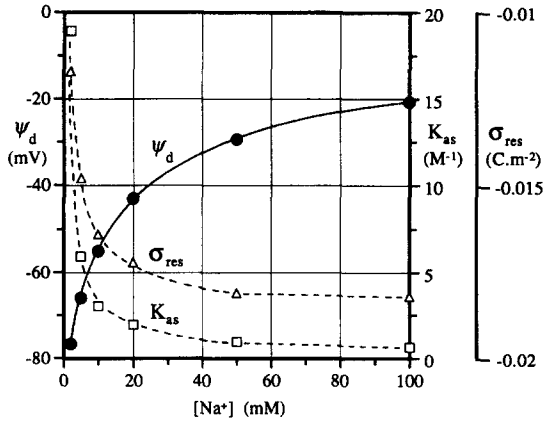

Fig. 5. Effect of Na^+ concentration on the interfacial potential (ψ_d) of galacto/sulfolipid lipisomes. The medium was as in Fig. 3, except that the pH was 9.1; the liposomes contained 10% SQDG. ψ_d (●) was calculated from the pK_a shifts observed with the probe U-2. K_{as} (□) and σ_{res} (△, the residual charge density after Na^+ binding) were derived from simulation of the Gouy-Chapman-Stern relations (also entered in the simulation protocol were the parameters: $\sigma_{max} = -0.0212284$ C m^{-2} for 10% SQDG; SQDG sulfonic acid group $pK_a = -3$; $d_s = 0.15$ nm; valency = 1).

3.6. Binding and dimerization of the monovalent amphiphilic cation acridine orange

In view of the results obtained with the inorganic alkali metal cations it was of interest to compare these with the effects of binding of monovalent aromatic cations to the liposomes. For this purpose we studied the behavior of the aminoacridine dye acridine orange (AO). This compound is particularly useful for accurate binding studies because its binding to negatively charged membranes and biopolymers is exactly monitored by the fractional monomer fluorescence quenching, and dimer formation upon binding can be directly followed from its red-shifted fluorescence at room temperature [28]. For appreciable binding of cationic aminoacridines to membranes the presence of negatively charged groups is essential, even at a pH where most of the compound is uncharged [36]. Their sigmoidal binding pattern can be attributed to cooperative interaction between aminoacridine dimers and the array of negative sites. Dimer formation in chloroplasts was earlier reported for AO, Atebrin (Quinacrine) and 9-amino-6-chloro-2-methoxyacridine (ACMA) [28], and in more detail for 9-aminoacridine [37]. Fig. 7A shows the AO monomer fluorescence quenching as function of added AO concentration in 5% and 10% SQDG-containing galacto/sulfolipid LUVETs. The quenching plots clearly titrate the num-

ber of available negative sites in both liposome preparations. AO dimerization (Fig. 7B) occurs simultaneously with the monomer quenching (after saturation AO dimerization gradually continues as it does in aqueous solution).

The presence of AO dimers after binding to liposomes was also confirmed by fluorescence lifetime measurements. In the μM concentration range the AO monomer lifetime is dominant in aqueous medium and was found to be 1.78 ± 0.07 ns, while at concentrations above 0.5 mM the lifetime of the dimer of 2.85 ± 0.12 ns is in evidence. The dimer lifetime increases when AO is bound to the SQDG-containing liposomes and also with increasing fraction of negatively charged lipid. With 5% SQDG liposomes at pH 9.1 the AO (20 μM) lifetimes for monomer and dimer were 1.90 ± 0.01 ns and 3.59 ± 0.03 ns, respectively; at 20% SQDG and 40 μM AO the respective values were 1.84 ± 0.05 ns and 4.55 ± 0.18 ns. These values are comparable with the AO lifetimes observed in SDS micelles [38]. Multi-component analysis of the fluorescence decay profiles in liposomes indicated an additional lifetime of about 14 ns, presumably originating from higher AO aggregates, but this component fraction never exceeded 2.5%.

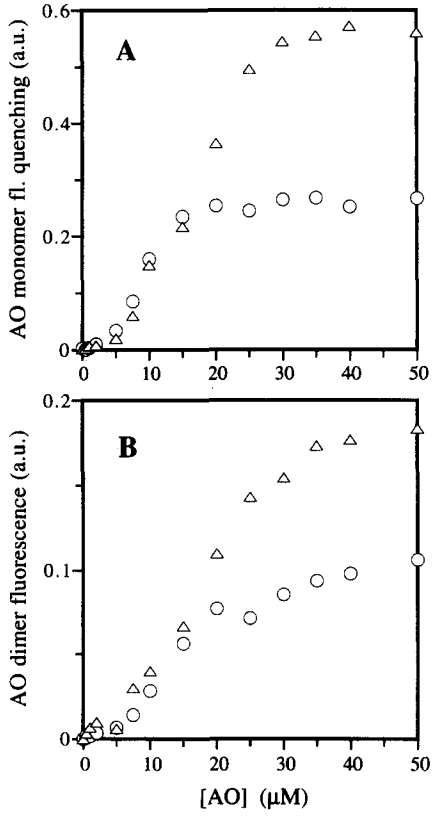

Fig. 7. AO monomer and dimer fluorescence changes in galactolipid/sulfolipid liposomes. Incubation conditions were as in Fig. 1, except that pH was 9.1. A: AO monomer excitation and emission wavelengths were set at 492 and 535 nm, respectively. B: AO dimer excitation and emission wavelengths were set at 450 and 620 nm, respectively. Liposomes contained 5% SQDG (○) or 10% SQDG (△).

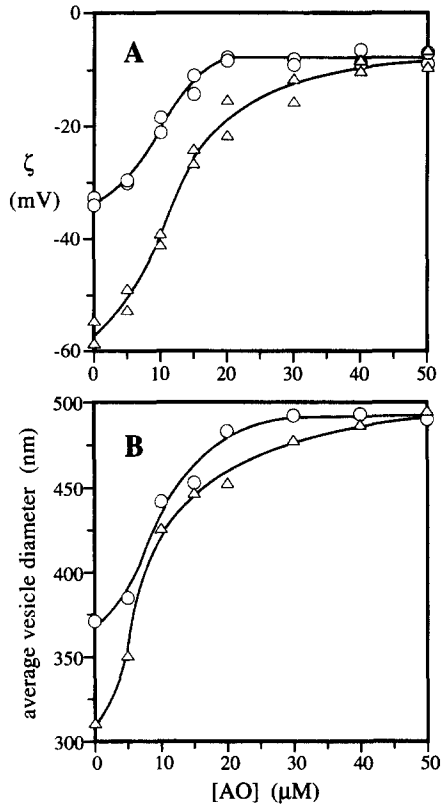

Fig. 8. Acridine orange effects on electrokinetic (ζ) potential (A) and average vesicle diameter (B) in galacto/sulfolipid liposomes. The incubation conditions and preparations were the same as in Fig. 7. Liposomes contained 5% SQDG (○) or 10% SQDG (△).

The effects of AO binding on ζ potential and vesicle size are shown in Fig. 8. The ζ potentials of 5% and 10% SQDG liposomes are effectively reduced to a constant (but non-zero) level at their respective saturating AO concentrations, and the curves are also slightly sigmoidal (Fig. 8A). AO binding also eliminates the vesicle size decrease brought about in 10 mM KCl and even produces the larger sizes typical for uncharged liposomes at low pH (Fig. 8B, compare Fig. 2). The divalent AO dimer cation apparently causes vesicle aggregation and/or fusion, and behaves similar to mM concentrations of Ca^{2+}. Liposome-bound aminoacridines can be rapidly released by Ca^{2+} [39] which also strongly indicates a peripheral location of these large and flat amphiphilic cations.

4. Discussion

4.1. Model membranes and interfacial potential determinations

Both types of LUVETs employed in this study display interfacial potentials (pH ≥ 7) consistent with the values expected for the lipid mixtures containing different fractions of monovalent negatively charged lipids. Also with

respect to the vesicle size measurements and cation perturbations, both the phospholipid and galacto/sulfolipid, as well as the PC/PS liposomes behave very similarly. This is somewhat surprising in view of their different lipid head-group structure and orientation. The determinations of ψ_d by the probe U-6 and of ζ potential by dynamic light scattering were accurate enough to study the small differential effects of alkali metal ions on these potentials at the low charge density range typical for biological membranes. Although in this range the surface charges are discrete rather than uniformly smeared, the observed (average) potentials still fit Gouy-Chapman-Stern theory [40]. Our data obtained with the probe U-6 also indicate that the less fixed 'ψ_0 probe' 2-(*p*-toluidinyl)-naphthalene-6-sulfonate (TNS), used by Eisenberg et al. [13], has indeed the assumed (average) sensor position.

4.2. Alkali metal ion association and shear boundary distance

The effects of alkali metal ions on ψ_d and the derived K_{as} values are in general agreement with the results of Eisenberg et al. [13] and Ermakov [29], based on ζ potential measurements with large multilamellar and small sonicated vesicles composed of different lipids (notably PS). The K_{as} values (Table 1) show a clear distinction between the Li^+-Na^+ and K^+-Cs^+ groups, and this is more pronounced for the galacto/sulfolipid vesicles. Our observation that vesicle sizes are the same in 10 mM Na^+ with or without 150 mM K^+, is in harmony with a prediction by Plesner and Michaeli [41] that in the case of mixed electrolytes (below a critical potential) cations with smaller (nonhydrated) ionic radii will be selectively adsorbed to a charged surface, almost completely excluding the larger ones, even at much higher concentrations of the latter.

By combining the K_{as} values for Li^+, Na^+, K^+, and Cs^+ with the ζ potentials, we obtained similar distances (about 0.2 nm) for the hydrodynamic plane of shear for all ions, at $\geq$ 100 mM, in accordance with Eisenberg et al. [13]. However, at lower concentrations (notably 10 mM), i.e. at increased Debye length, the shear boundary distance detectably increases, and more so in the presence of Li^+ or Na^+ (about 0.39 nm) than with K^+ or Cs^+ (about 0.31 nm), in agreement with early model studies on colloidal particles [19]. The explanation of the more substantial shear layer in the presence of hydration-promoting cations is hampered by great uncertainties about the nature of the hydration layer [16]. In line with Kita et al. [11], the 'structure-making' effects of Li^+ and Na^+ (and H_3O^+) may arise from the phenomenon of preferential hydration as a result of a non-uniform distribution of ions across the hydration layer, resulting in an interfacial tension. This tension would cause changes in the interfacial area, and hence of the shear layer thickness. In the classical double-layer hypothesis the preferential association of hydration-promoting ions may be viewed as a 'constructive interaction' between their hydration shells and that of the charged surface [42]. A hydration layer of about 0.4 nm thickness would roughly accomodate two, not necessarily continuous, layers of 'structured' water molecules, including adsorbed cations. Small hydrated ions can fit well within the water lattice without disrupting the hydrogen-bond network. A PC/water interfacial hydration layer of this size would contain about 20 bound water molecules per PC head group [23]. Bérubé and De Bruyn [42] suggested that the hydrodynamic plane of shear may coincide with a 'thawed region' of high structural disorder and relatively low viscosity between the ordered hydration layer and bulk water. Regardless of the exact molecular mechanism, it is likely that differential cation perturbations of the hydration layer will also affect hydrodynamic properties.

4.3. Membrane curvature and lipid asymmetry

The differential behavior of alkali metal ions is most pronounced with regard to their effects on membrane curvature (Figs. 2 and 6). It is likely that during the extrusion process the liposomes undergo a transient destabilization that allows the lipids to rearrange themselves into the energetically most favourable position. The remarkable decrease of vesicle size, observed in the presence of low K^+ or Cs^+ concentrations, indicates that the membranes are less stable than in the presence of the stronger associating Li^+ and Na^+ which apparently prevent major curvature changes. Asymmetric distribution of the charged lipids in favour of the outer leaflet is indicated by the AO fluorescence titrations of the galacto/sulfolipid vesicles (in 10 mM KCl). Lentz [43] suggested that dehydration leads to asymmetry in the lateral pressure in each leaflet. At higher salt concentrations the charge screening causes an additional compensation, but this is less effective than direct association of the cation with the negative sites. Mattai et al. [44] studied the interaction of several cations with PS monolayers and bilayers in relation to lipid head-group dynamics, surface area, and chain type and packing. Except for the Na^+ effects, our results are in general agreement with their studies. Disaccharides also contribute to membrane hydration; sucrose was found to partly prevent curvature changes (Fig. 6). The lipid-bound galactosyl moieties of MGDG and DGDG may provide localized groups which promote interfacial stabilization [45,46].

4.4. Behavior of the large amphiphilic cation acridine orange

Like other aminoacridines, AO strongly interacts with the negative binding sites in its dimeric form [28,37]. The AO dimer is of the sandwich type, with the positively charged ring-nitrogens oppositely directed [26]. The dimer conformation is mainly stabilized by hydrogen bonds, Van der Waals' interactions and additional hydration. Dimer formation only occurs in aqueous solution and is promoted by existing hydration layers along interfaces or polymers

and by Na^+ or Mg^{2+} ions, and reversed by urea [15]. Detection of aminoacridine dimerization is therefore indicative for the hydrated nature of its environment. The perturbing effects of AO on the liposome interface are qualitatively similar to those of Na^+, K^+, H_3O^+, and divalent cations, but the effects are more drastic (note that we have only studied the post-extrusion, i.e. external, effects of AO on the interfacial properties).

4.5. Physiological implications

The results of this study may contribute to better understanding physiological differences between Na^+ and K^+ interactions with biological membranes. We suggest that the differential effects of monovalent cations on membrane surface properties are related to their own hydration tendency and potency to stabilize or destabilize the hydrogen-bond network along membrane surfaces. Biomembranes have to be capable of rearrangements to allow their functionally important dynamics. This implies that their interfacial structure should neither be too labile, nor too stable. It appears that the hydration state of the membrane is directly or indirectly linked to the local activity and type of counterion, interfacial potential, lipid headgroup orientation, hydrocarbon chain saturation [5,8,47], hexagonal phase-forming propensity of lipids [48], bilayer adhesion/fusion [49,50], but not to the lipid order [51]. Ion-transporting proteins cause local redistributions of ions and often generate electric fields which will affect the charge orientation and dielectric constant in the interfaces [5]. The existence of lateral heterogeneity of proteins and lipids, often existing in special aggregates, and the spatial variations in membrane curvature (e.g., in chloroplasts, mitochondria, and plasma membranes of many specialized cell types) would suggest that the differential monovalent cation effects may be of physiological significance by modulating the structure and dynamics of such local areas of biomembranes.

Acknowledgements

Prof. Stuart McLaughlin is kindly acknowledged for suggesting the new estimations of the shear boundary distances, and for critical comments. We are also grateful to Prof. Gus Somsen for instructive discussions on hydration phenomena. The development of membrane probes was supported in part by the Netherlands Technology Foundation (STW) with financial aid from the Netherlands Organization for Scientific Research (NWO).

References

[1] McLaughlin, S. (1977) Curr. Top. Membr. Transp. 9, 71–144.
[2] McLaughlin, S. (1989) Ann. Rev. Biophys. Biophys. Chem. 18, 113–136.
[3] Barber, J. (1980) Biochim. Biophys. Acta 594, 253–308.
[4] Pal, R., Petri, W.A., Ben-Yashar, V., Wagner, R.R. and Barenholz, Y. (1985) Biochemistry 24, 573–581.
[5] Scherer, P.G. and Seelig, J. (1989) Biochemistry 28, 7720–7728.
[6] Shin, Y.-K. and Hubbell, W.L. (1992) Biophys. J. 61, 1443–1453.
[7] Luzar, A., Svetina, S. and Žekš, B. (1985) J. Chem. Phys. 82, 5146–5154.
[8] Slater, S.J., Ho, C., Taddeo, F.J., Kelly, M.B. and Stubbs, C.D. (1993) Biochemistry 32, 3714–3721.
[9] Rand, R.P. (1992) Science 256, 618.
[10] Rand, R.P. and Parsegian, V.A. (1989) Biochim. Biophys. Acta 988, 351–376.
[11] Kita, Y., Arakawa, T., Lin, T.-Y. and Timasheff, S.N. (1994) Biochemistry 33, 15178–15189.
[12] Epand, R.M. and Bryszewska, M. (1988) Biochemistry 27, 8776–8779.
[13] Eisenberg, M., Gresalfi, T., Riccio, T. and McLaughlin, S. (1979) Biochemistry 18, 5213–5223.
[14] Franks, F. (1975) Water - A Comprehensive Treatise, Vol. 4: Aqueous Solutions of Amphiphiles and Macromolecules, Plenum Press, New York.
[15] Conway, B.E. (1981) Ionic Hydration in Chemistry and Biophysics, Elsevier, Amsterdam.
[16] Franks, F. and Mathias, S.F. (1982) Biophysics of Water, John Wiley and Sons, Chichester.
[17] Samoilov, O.Y. (1972) in Water and Aqueous Solutions (Horne, R.A., ed.), pp. 597–612, Wiley Interscience, New York.
[18] Desnoyers, J.E. and Perron, G. (1972) J. Solut. Chem. 1, 199–212.
[19] Gargallo, L., Sepulveda, L. and Goldfarb, J. (1969) Kolloid Z. Z. Polym. 229, 51–54.
[20] Kraayenhof, R., Sterk, G.J. and Wong Fong Sang, H.W. (1993) Biochemistry 32, 10057–10066.
[21] Hof, M., Hutterer, R., Pérez, N., Ruf, H. and Schneider, F.W. (1994) Biophys. Chem. 52, 165–172.
[22] Hauser, H. (1975) in Water - A Comprehensive Treatise, Vol. 4: Aqueous Solutions of Amphiphiles and Macromolecules (Franks, F., ed.), Plenum Press, New York.
[23] Rigaud, J.L. and Gary-Bobo, C.M. (1977) Biochim. Biophys. Acta, 469, 246–256.
[24] Israelachvili, J.N. and Pashley, R.M. (1982) in Biophysics of Water (Franks, F. and Mathias, S.F., eds.), Wiley, Chichester.
[25] Fromherz, P. (1989) Methods Enzymol. 171, 376–387.
[26] Zanker, V. (1952) Z. Physik. Chem. 199, 225–258.
[27] Mayer, L.D., Hope, M.J. and Cullis, P.R. (1986) Biochim. Biophys. Acta 858, 161–168.
[28] Torres-Pereira, J.M.G., Wong Fong Sang, H.W., Theuvenet, A.P.R. and Kraayenhof, R. (1984) Biochim. Biophys. Acta 767, 295–303.
[29] Ermakov, Y.A. (1990) Biochim. Biophys. Acta 1023, 91–97.
[30] Makino, K., Yamada, T., Kimura, M., Oka, T., Ohshima, H. and Kondo, T. (1991) Biophys. Chem. 41, 175–183.
[31] Träuble, H. and Eibl, H. (1974) Proc. Natl. Acad. Sci. USA 71, 214–219.
[32] Winiski, A.P., Eisenberg, M., Langner, M. and McLaughlin, S. (1988) Biochemistry 27, 386–392.
[33] Langner, M., Cafiso, D., Marčelja, S. and McLaughlin, S. (1990) Biophys. J. 57, 335–349.
[34] Bryszewska, M. and Epand, R.M. (1988) Biochim. Biophys. Acta 943, 485–492.
[35] Fabrie, C.H.J.P., De Kruijff, B. and De Gier, J. (1990) Biochim. Biophys. Acta 1024, 380–384.
[36] Kraayenhof, R. (1980) Methods Enzymol. 69, 510–520.
[37] Grzesiek, S. and Dencher, N.A. (1988) Biochim. Biophys. Acta 938, 411–424.
[38] Miyoshi, N., Hara, K. Yokoyama, I., Tomita, G. and Fukuda, M. (1988) Photochem. Photobiol. 47, 685–688.
[39] Kraayenhof, R. and Arents, J.C. (1977) in Electrical Phenomena at

the Biological Membrane Level (Roux, E., ed.), pp. 493–504, Elsevier, Amsterdam.
[40] Peitzsch, R.M., Eisenberg, M., Sharp, K.A. and McLaughlin, S. (1995) Biophys. J. 68, 729–738.
[41] Plesner, I.W. and Michaeli, I. (1974) J. Chem. Phys. 60, 3016–3024.
[42] Bérubé, Y.G. and De Bruyn, P.L. (1968) J. Colloid Interface Sci. 28, 92–105.
[43] Lentz, B.R. (1994) Chem. Phys. Lipids 73, 91–106.
[44] Mattai, J., Hauser, H., Demel, R.A. and Shipley, G.G. (1989) Biochemistry 28, 2322–2330.
[45] Jarrell, H.C., Jovall, P.Å., Giziewicz, J.B., Turner, L.A. and Smith, I.C.P. (1987) Biochemistry 26, 1805–1811.
[46] Park, Y.S. and Huang, L. (1992) Biochim. Biophys. Acta 1112, 251–258.
[47] Macdonald, P.M., Leisen, J. and Marassi, F.M. (1991) Biochemistry 30, 3558–3566.
[48] Epand, R.M. and Leon, B.T.-C. (1992) Biochemistry 31, 1550–1554.
[49] Burgess, S.W., McIntosh, T.J. and Lentz, B.R. (1992) Biochemistry 31, 2653–2661.
[50] Lehtonen, J.Y.A. and Kinnunen, P.K.J. (1994) Biophys. J. 66, 1981–1990.
[51] Ho, C., Slater, S.J. and Stubbs, C.D. (1995) Biochemistry 34, 6188–6195.